AGU PUBLICATIONS

Geochemistry, Geophysics, Geosystems

RESEARCH ARTICLE
10.1002/2014GC005657

Key Points:
- Madeira Island emerged by rapid uplift at 7.0–5.6 Ma before shield volcanism
- Uplift is corroborated by marine sediments at 320–430 m in elevation
- Island emergence by uplift might be common on slow-moving plates

Supporting Information:
- Readme
- Dataset S1

Correspondence to:
R. S. Ramalho,
ric.ramalho@bristol.ac.uk

Citation:
Ramalho, R. S., A. Brum da Silveira, P. E. Fonseca, J. Madeira, M. Cosca, M. Cachão, M. M. Fonseca, and S. N. Prada (2015), The emergence of volcanic oceanic islands on a slow-moving plate: The example of Madeira Island, NE Atlantic, *Geochem. Geophys. Geosyst.*, *16*, 522–537, doi:10.1002/2014GC005657.

Received 11 NOV 2014
Accepted 26 JAN 2015
Accepted article online 4 FEB 2015
Published online 24 FEB 2015

The emergence of volcanic oceanic islands on a slow-moving plate: The example of Madeira Island, NE Atlantic

Ricardo S. Ramalho[1,2], António Brum da Silveira[3,4], Paulo E. Fonseca[3,4], José Madeira[3,4], Michael Cosca[5], Mário Cachão[3,4], Maria M. Fonseca[6], and Susana N. Prada[7,8]

[1]School of Earth Sciences, University of Bristol, Bristol, UK, [2]Lamont-Doherty Earth Observatory at Columbia University, Palisades, New York, USA, [3]Departamento de Geologia, Faculdade de Ciências, Universidade de Lisboa, Lisboa, Portugal, [4]Instituto Dom Luiz, Faculdade de Ciências, Universidade de Lisboa, Lisboa, Portugal, [5]U.S. Geological Survey, Denver Federal Center, Denver, Colorado, USA, [6]Instituto Investigação Científica Tropical/Bio Trop—Instituto Superior de Agronomia, Lisboa, Portugal, [7]Universidade da Madeira, Madeira, Portugal, [8]Departamento de Ciências Exactas e da Engenharia, Centro de Vulcanologia e Avaliação de Riscos Geológicos da Universidade dos Açores, Ponta Delgada, Portugal

Abstract The transition from seamount to oceanic island typically involves surtseyan volcanism. However, the geological record at many islands in the NE Atlantic—all located within the slow-moving Nubian plate—does not exhibit evidence for an emergent surtseyan phase but rather an erosive unconformity between the submarine basement and the overlying subaerial shield sequences. This suggests that the transition between seamount and island may frequently occur by a relative fall of sea level through uplift, eustatic changes, or a combination of both, and may not involve summit volcanism. In this study, we explore the consequences for island evolutionary models using Madeira Island (Portugal) as a case study. We have examined the geologic record at Madeira using a combination of detailed fieldwork, biostratigraphy, and $^{40}Ar/^{39}Ar$ geochronology in order to document the mode, timing, and duration of edifice emergence above sea level. Our study confirms that Madeira's subaerial shield volcano was built upon the eroded remains of an uplifted seamount, with shallow marine sediments found between the two eruptive sequences and presently located at 320–430 m above sea level. This study reveals that Madeira emerged around 7.0–5.6 Ma essentially through an uplift process and before volcanic activity resumed to form the subaerial shield volcano. Basal intrusions are a likely uplift mechanism, and their emplacement is possibly enhanced by the slow motion of the Nubian plate relative to the source of partial melting. Alternating uplift and subsidence episodes suggest that island edifice growth may be governed by competing dominantly volcanic and dominantly intrusive processes.

1. Introduction

The emergence of Capelinhos volcano (Azores, Portugal) in 1957, and especially the emergence of Surtsey Island (Iceland) in 1961, provided some of the first modern scientific accounts of volcanic seamounts that rose above sea level by means of summit eruptions to form precursory islands. As a consequence, the term "surtseyan" entered the volcanological lexicon and is associated with hydromagmatic, explosive eruptive styles typical of a volcanic system whose vent is located in shallow waters [*Thorarinsson*, 1967a, 1967b]. Additionally, the eruptions at Surtsey and Capelinhos also provided insight into the transition between emergent and subaerial shield-building stages of island evolution. Both volcanoes started as submarine structures (effusive in the case of Surtsey). Submarine eruptions gradually increased in explosivity as the edifices shoaled, due to higher magma fragmentation with decreasing water/magma ratios and hydrostatic pressures [*Machado*, 1962; *Zbyszewski and Ferreira*, 1962; *Wohletz and McQueen*, 1984; *Moore*, 1985; *Kokelaar*, 1986]. A series of steam-driven blasts followed, disrupting the sea surface and producing large quantities of tephra that accumulated around the vents to form cones or rings that eventually breached the sea surface [*Machado*, 1962; *Zbyszewski and Ferreira*, 1962; *Thorarinsson*, 1967a; *Kokelaar*, 1983; *Moore*, 1985]. As these submarine tephra cones built up above sea level, their vents were gradually isolated from seawater resulting in vigorous sets of uprush eruptions that rapidly and drastically declined to give way to strombolian eruptions when water in the system was completely (or almost completely) expended [*Machado*, 1962;

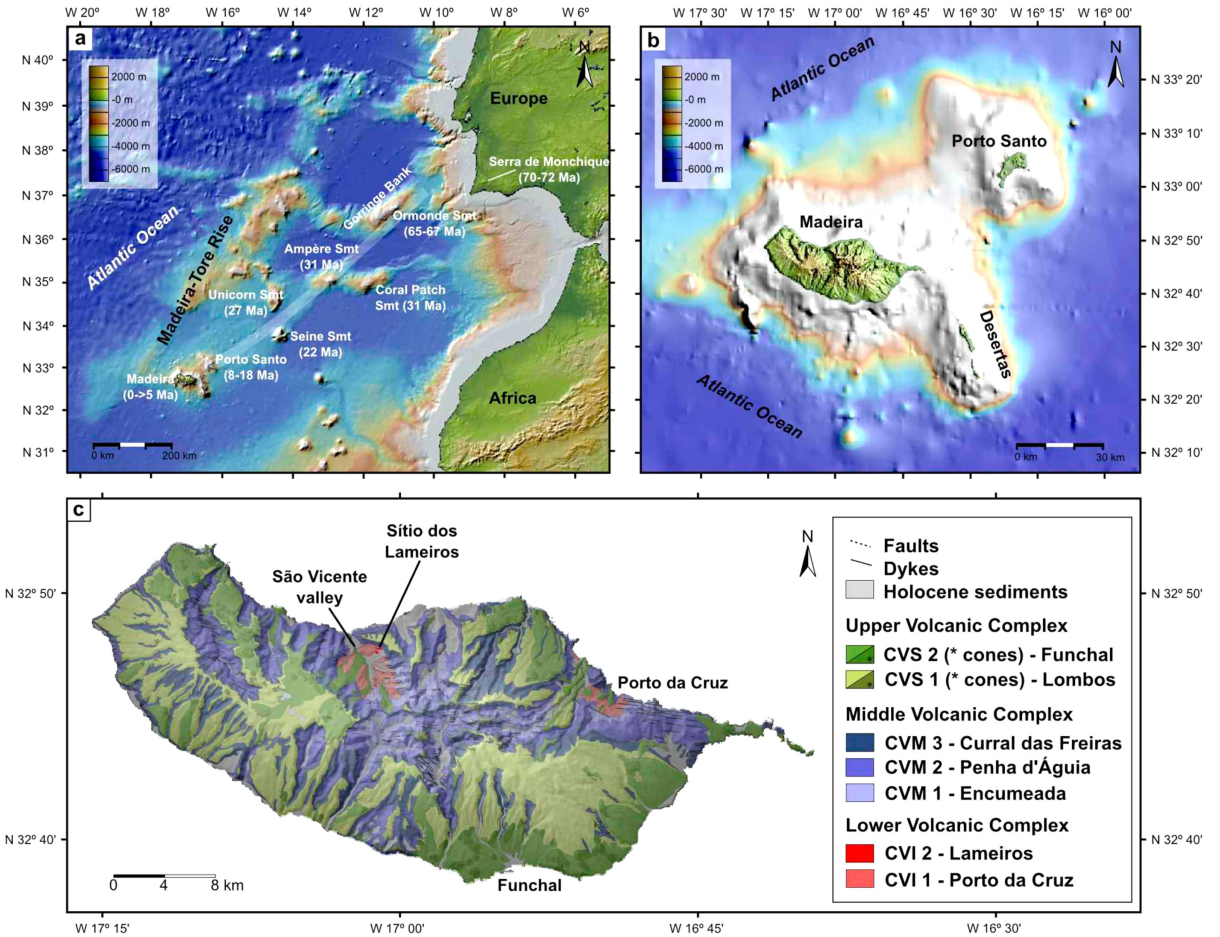

Figure 1. Location and geologic maps of Madeira Island. (a) Location of Madeira Archipelago at the end of the hot spot track as inferred by *Geldmacher et al.* [2005]. (b) Location of Madeira Island relative to nearby Porto Santo and Desertas islands. Note the elongated shield-morphology of Madeira island edifice. (c) Simplified geologic map of Madeira Island [after *Brum da Silveira et al.*, 2010a, 2010b]. Note the position of the basal unit CVI1 within São Vicente valley and the area around Porto da Cruz, as well as the position of the marine sediments (CVI2) at Sítio dos Lameiros. Basemaps created from Global Multi-Resolution Topography (GMRT) Synthesis [*Ryan et al.*, 2009], using GeoMapApp (http://www.geomapapp.org).

Thorarinsson, 1967a; *Moore*, 1985; *Sohn*, 1995]. Soon, the onset of subaerial effusive activity followed, leading to the formation of lava flow caps (less prominently on Capelinhos) that consolidated and protected the island edifices from marine erosion and led to longer island survival [*Thordarson and Sigmarsson*, 2009].

Since the events at Capelinhos and Surtsey, it is inferred that most ocean island volcanoes experienced a surtseyan phase during their emergence and that the products of this eruptive stage (even if partially eroded) lie buried deep under the large subaerial edifices that we see today, and in most islands made even more inaccessible by subsidence and rising Holocene sea level. However, the geological record from several uplifted and eroded islands in the Atlantic does not seem to exhibit the remains of a surtseyan phase [see *Staudigel and Schmincke*, 1984; *Schmidt and Schmincke*, 2000, 2002; *Ramalho*, 2011; *Johnson et al.*, 2014], suggesting that island emergence may take place through a process other than summit volcanism. This process of emergence must involve a relative fall in sea level through either uplift, eustatic changes, or a combination of both between eruptive periods [*Ramalho et al.*, 2013]. Such a process is suggested by the presence of an irregular erosive unconformity between the seamount products and subaerial shield sequences that compose these island edifices [e.g., *Staudigel and Schmincke*, 1984; *Madeira et al.*, 2010; *Johnson et al.*, 2014]. However, little is known about this process of island emergence, its timing, and the magnitude of the vertical movements involved. This study aims to document one such case—Madeira Island—in order to gain better insight on island emergence and early subaerial development stages of ocean island volcanoes, particularly those that exhibit long but intermittent eruptive lives as observed for edifices located on slow-moving plates [*Schmincke*, 2004; *Ramalho*, 2010, 2011; *Ramalho et al.*, 2013].

2. Geological Setting

Madeira Island is located in the NE Atlantic, between latitudes 32°38′N and 32°52′N, and approximately 700 km to the west of Africa (Figure 1a). The island is the emerged part of a large volcanic edifice that rises almost 6 km from the surrounding seafloor, from the −4000 m isobath to 1861 m above present sea level (a.p.s.l). The island is a deeply dissected shield-volcano elongated in a E-W direction, extending to 57 km in maximum length and 21 km of maximum width. Madeira is generally considered the result of a hotspot that impinged the slow-moving African (Nubian) plate, leaving a possible hotspot track (see Figure 1a) that extends northeast to Porto Santo Island (8–18 Ma) and the seamounts of Seine (22 Ma), Unicorn (27 Ma), Ampere and Coral Patch (31 Ma), and Ormonde (65–67 Ma) [*Ferreira*, 1985; *Ferreira et al*., 1988; *Geldmacher et al*., 2005]. The nearby island of Porto Santo (Figure 1b) corresponds to a volcano that shoaled and emerged around 11–14 Ma by means of hydromagmatic volcanic activity, and was subsequently uplifted by at least 330–365 m [*Schmidt and Schmincke*, 2002; *Mata et al*., 2013].

The subaerial history of Madeira Island is inferred to extend from the Late Miocene or Early Pliocene, to the Holocene. Previous workers suggested a complex intermittent magmatic life and reported ages ranging between 5.6 Ma and 6.5 ka [*Watkins and Abdel-Monem*, 1971; *Feraud et al*., 1981; *Ferreira*, 1985; *Ferreira et al*., 1988; *Mata et al*., 1995; *Mata*, 1996; *Geldmacher and Hoernle*, 2000; *Geldmacher et al*., 2000; *Ech-chakrouni*, 2004; *Klügel et al*., 2009]. As previous studies note, the absence of obvious submarine volcanic products on the exposed Madeira shield edifice is noteworthy (except for very recent littoral volcanism). However, the presence of in-sequence marine sediments exposed at Sítio dos Lameiros—a locality within São Vicente Valley and at 300–450 m in elevation (Figure 1c)—is well documented [e.g., *Romariz*, 1971a, 1971b; *Mitchell-Thomé*, 1974; *Zbyszewski et al*., 1975; *Mata*, 1996] and recognized as possible evidence for a complex history of vertical movements affecting the island edifice [*Mata*, 1996]. The stratigraphic reconciliation between the presence of marine sediments at those elevations and the apparent absence of submarine volcanic morphologies anywhere on the island is still largely unresolved, a fact mainly attributed to the scarcity of exposures and the lack of detailed island-scale stratigraphic studies. Consequently, little is known about the mechanism(s) that resulted in these marine sediments arriving at their present position.

A recent detailed geological survey of Madeira Island took place between 2002 and 2010, from which two 1/50000 scale geologic maps and an accompanying memoir were published [see *Brum da Silveira et al*., 2010a, 2010b, 2010c] (Figure 1c). The field observations conducted during this survey, as well as the stratigraphic information derived from these observations, constitute the basis for the present study. As such, *Brum da Silveira et al*. [2010a, 2010b, 2010c] concluded that the island's stratigraphic succession comprises seven formal unconformity-bounded units/formations (from the base to the top, Figure 1c): Porto da Cruz (CVI1) and Lameiros (CVI2) Fms within the Lower Volcanic Complex (Complexo Vulcânico Inferior); Encumeada (CVM1), Penha D'Águia (CVM2), and Curral das Freiras (CVM3) Fms within the Middle Volcanic Complex (Complexo Vulcânico Médio); and Lombos (CVS1) and Funchal (CVS2) Fms within the Upper Volcanic Complex (Complexo Vulcânico Superior). The Porto da Cruz Fm, composed of strongly altered hydrovolcanic rocks, possibly relates to the seamount building volcanic stage and is locally covered by marine sedimentary deposits of the Lameiros Fm. The Middle Volcanic Complex, which lies above the the Lower Volcanic Complex, constitutes the largest portion of Madeira's subaerial volume and comprises three unconformity-bounded units. These formations comprise successions of basaltic lava flows and tephra layers, with interbedded epiclastic deposits, accumulated during the main subaerial shield-building stage of island evolution. Finally, the Lombos and Funchal Fms correspond to, respectively, a capping and a posterosional, topography filling volcanic stages.

3. Material and Methods

3.1. Characterization of Geological Units and Stratigraphic Contacts

The nature and geometry of the contacts between the geological units, and the nature of these units themselves, were studied in detail in the field using direct observations and geological mapping at different scales (1/10000 and 1/50000). Geological units were defined as individual volcanostratigraphic entities, reflecting distinct phases in the evolution of the island edifice bounded by regional unconformities [*Brum da Silveira et al*., 2010c].

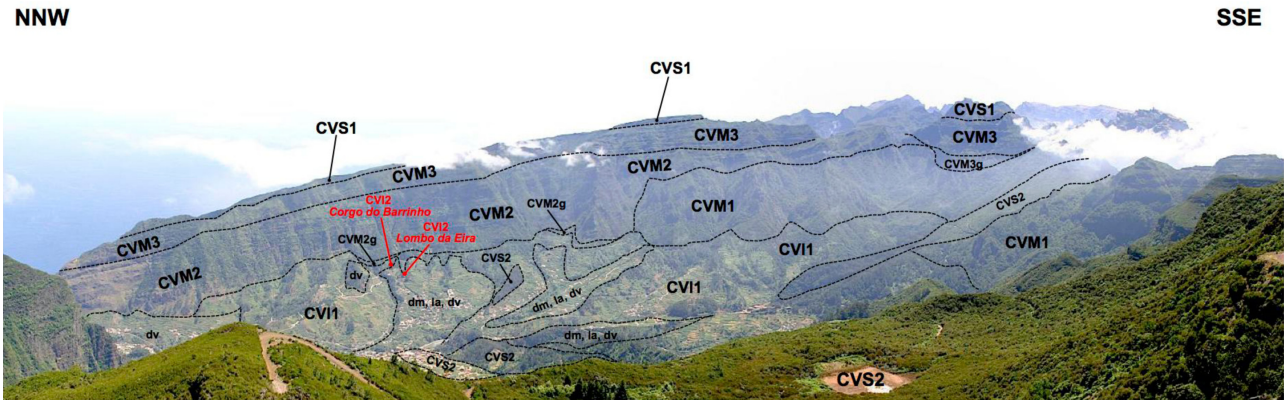

Figure 2. Approximate boundaries between main geological units along the eastern wall of São Vicente Valley. Please note the location of Lameiros outcrops (CVI2, in red) wedged in between Porto da Cruz Fm (CVI1) and the massive effusive sequence of Penha D'Águia (CVM2). Note also that Encumeada (CVM1) locally ends abruptly at the upper reaches of the valley (CVI1, Porto da Cruz Fm; CVI2, Lameiros Fm; CVM1, Encumeada Fm; CVM2g, basal conglomerates of Penha D'Águia Fm; CVM2, Penha D'Águia Fm; CVM3g, basal conglomerates of Curral das Freiras Fm; CVM3, Curral das Freiras Fm; CVS1, Lombos Fm; CVS2, Funchal Fm; dv, slope deposits; dm, landslide deposits; la, lahar deposits).

3.2. Marine Sediment Characterization and Paleoenvironmental Reconstructions

The marine sediments at Sítio dos Lameiros (Figure 2) are exposed along Corgo do Barrinho creek (the largest exposure) and at Lombo da Eira (a residual outcrop). Strip logs for stratigraphic sections were assembled along a composite vertical profile following the Corgo do Barrinho stream bed. Care was taken to register changes in facies and occurrences of fossils. Variations in fossil content were noted and representative examples were photographed. Paleoenvironmental reconstructions were based on characteristic facies and macrofossil content. Additionally, three sets of samples were collected at the lower, intermediate, and upper portions of the sedimentary sequence for calcareous nannofossil screening. Preparation for calcareous nannofossil observations, by petrographic microscope, followed the optimized procedure described in *Johnson et al*. [2014]. Calcareous nannofossil taxonomy follows criteria standardized by *Perch-Nielsen* [1985] and *Bown* [1998].

3.3. X-Ray Diffraction

X-ray diffraction (XRD) was used to investigate the hydrovolcanic nature of both the parent rock and the alteration affecting CVI1 lithologies, and in particular to test the presence of vitreous/amorphous material and signs of palagonitization. Vitreous material is a common constituent of hydrovolcanic rocks and palagonite is a common hydrated first alteration product of mafic glass when exposed to water and so it is usually associated with subaqueous basaltic volcanic successions [*Bonatti*, 1965; *Summers*, 1976; *Furnes*, 1984; *Zhou et al*., 1992; *Stroncik and Schmincke*, 2002; *Michalski et al*., 2005; *Achilles et al*., 2013]. Two samples were collected at Porto da Cruz and subsequently analyzed. Additionally, an unaltered subaerial basalt from Cabo Girão was used as a control sample. The analyses were performed on a Philips PW1710 diffractometer, using the software PC-APD, version 3.6 (Philips Scientific). A "peak search" function was used to detect reflection angles 2θ and respective intensities, with "Minimum and Second Derivative of Peak." A copper anode was used as the X-ray radiation source (20 mA and 40 kV). Data were obtained using a continuous scan, between 2° and 65° 2θ, with a scanning speed of $0.02\theta s^{-1}$. Resulting diffractograms were analyzed with MacDiff (version 4.25, by *Petschick* [2004]), and feature in Appendix A (Figure A1).

3.4. Sample Collection for $^{40}Ar/^{39}Ar$ Geochronology

The outcrops at Sítio dos Lameiros were extensively reduced by historic mining to produce quicklime, limiting available sampling sites. Four targets were selected for sampling: two samples correspond to exposures interpreted as volcanic products underlying the sediments at Lombo da Eira, and two correspond to different basaltic clasts included within the upper portion of the main marine sediment exposure at Corgo do Barrinho (see Table 1 for sample reference, location and description). Sampling was also attempted where the volcanic deposits that cap the marine sediments are exposed, but it was not possible to recover samples pristine enough for geochronology. Samples were collected with a handheld gasoline diamond core drill. Drill cores were later cut into smaller pieces and the least altered samples were used for thin sections and geochronology.

Table 1. Summary of Sample Information for $^{40}Ar/^{39}Ar$ Geochronology

Sample ID	Geographic Coordinates (Lat/Lon WGS84)	Type
M-05	N32°47′44.2″W17°01′31.4″	Volcanics underlying the sediments
M-15	N32° 47′52.4″W17°01′22.5″	Basaltic cobble/boulder within marine sediments
M-18	N32° 47′44.3″W17°01′31.1″	Volcanics underlying the sediments
M-19	N32° 47′52.4″W17°01′22.5″	Basaltic cobble/boulder within marine sediments

3.5. Laser Step Heating $^{40}Ar/^{39}Ar$ Geochronology

The $^{40}Ar/^{39}Ar$ analyses were performed at the USGS in Denver, CO. Samples were prepared by crushing and isolating fresh rock fragments ($\sim$1 mm^3) free of obvious alteration. The rock fragments were washed in deionized water and together with standards, were irradiated for 2 MW h in the central thimble position of the USGS TRIGA reactor. Laser fusion of >10 individual Fish Canyon Tuff sanidine crystals (28.201 $\pm$ 0.046 Ma) [*Kuiper et al*., 2008] at each closely monitored position within the irradiation package resulted in neutron flux ratios reproducible to $\pm 0.25\%(2\sigma)$. Isotopic production ratios were determined from irradiated CaF_2 and KCl salts and for this study the following values were measured: $(^{36}Ar/^{37}Ar)_{Ca} = (2.45 \pm 0.05) \times 10^{-4}$; $(^{39}Ar/^{37}Ar)_{Ca} = (6.59 \pm 0.10) \times 10^{-4}$; and $(^{38}Ar/^{39}Ar)_{K} = (1.29 \pm 0.03) \times 10^{-2}$. Cadmium shielding during irradiation prevented any measurable $(^{40}Ar/^{39}Ar)_{K}$. The irradiated basalt samples and standards were loaded into numbered positions of a stainless steel planchette, placed into a laser sample chamber with an externally pumped ZnSe window, and evacuated to ultrahigh vacuum conditions in a fully automated stainless steel extraction line designed and built at the USGS in Denver. Using a 25 W CO_2 laser equipped with a beam homogenizing lens, the samples were incrementally heated and the liberated gas was expanded and purified by exposure to a cryogenic trap maintained at -135°C and two hot SAES^{TM} GP50 getters. Following purification, the gas was expanded online into a Mass Analyzer Products^{TM} 215-50 mass spectrometer in static mode and Ar isotopes were measured by peak jumping using an electron multiplier in analog mode. Data were acquired during 10 measurement cycles and time zero intercepts were determined by best fit linear and/or polynomial regressions to the data. Data were also corrected for the source mass discrimination (1.0045 amu) by regular measurement of pipetted atmospheric argon assuming an atmospheric $^{40}Ar/^{36}Ar$ value of 298.56 $\pm$ 0.31 [*Lee et al*., 2006]. The isotopic data were corrected for the laser extraction line and mass spectrometer blanks by applying a time-integrated blank value constructed from blanks analyzed before and after each sample. The decay constants tabulated in *Steiger and Jäger* [1977] were used for the age calculations.

4. Results

4.1. Evidence for a Submarine Volcanic Basement

The oldest stratigraphic unit in Madeira (Porto da Cruz Fm—CVI1) is only exposed within two regions in the northern half of Madeira Island, at Porto da Cruz and São Vicente valleys (see Figure 1c). At Porto da Cruz valley, CVI1 crops out from sea level up to 390 m in elevation, whereas in São Vicente valley it crops out from 70 to $\sim$800 m in elevation (Figure 2). In both areas the lithologies composing this unit are intensely altered to a distinctive clay-rich mass with a color ranging from orange/yellow to light brown, in which internal structures/textures are rarely discernible. However, in places where internal structures are perceptible, they mostly correspond to hyaloclastite and pillow breccias (see Figure 3a) and more rarely to massive lava flows. The distinctive alteration suggests a pervasive palagonitization [*Bonatti*, 1965; *Singer*, 1974; *Stroncik and Schmincke*, 2002; *Michalski et al*., 2005; *Brum da Silveira et al*., 2010c; *Achilles et al*., 2013]. X-ray diffractograms (samples PC-01 and PC-02, see Figure A1) are consistent with altered glass to amorphous material [*Stroncik and Schmincke*, 2002; *Achilles et al*., 2013] of basaltic composition. These diffractograms indicate the presence of saponite (a trioctahedral smectite), maghemite and hematite, phillipsite (a hydrated potassium, calcium and aluminum zeolite), opal and tridymite. These minerals are characteristic of seawater/basalt interaction and the corresponding palagonitization process, and are in stark contrast with the unaltered subaerial basalt of the control sample (sample MA-21, see Figure A1) that simply exhibits the peaks of basaltic mineralogy.

The hydrovolcanic products of CVI1 are intruded by a dense dyke swarm with an overall E-W trend. More voluminous masses of intrusive rocks also occur within this unit; for example, the small gabbroic plutons in the vicinity of Porto da Cruz and the trachyte plugs on the lower reaches of São Vicente Valley [see *Brum da Silveira et al*., 2010b]. Since these intrusive masses were exposed by erosion and mass wasting processes—

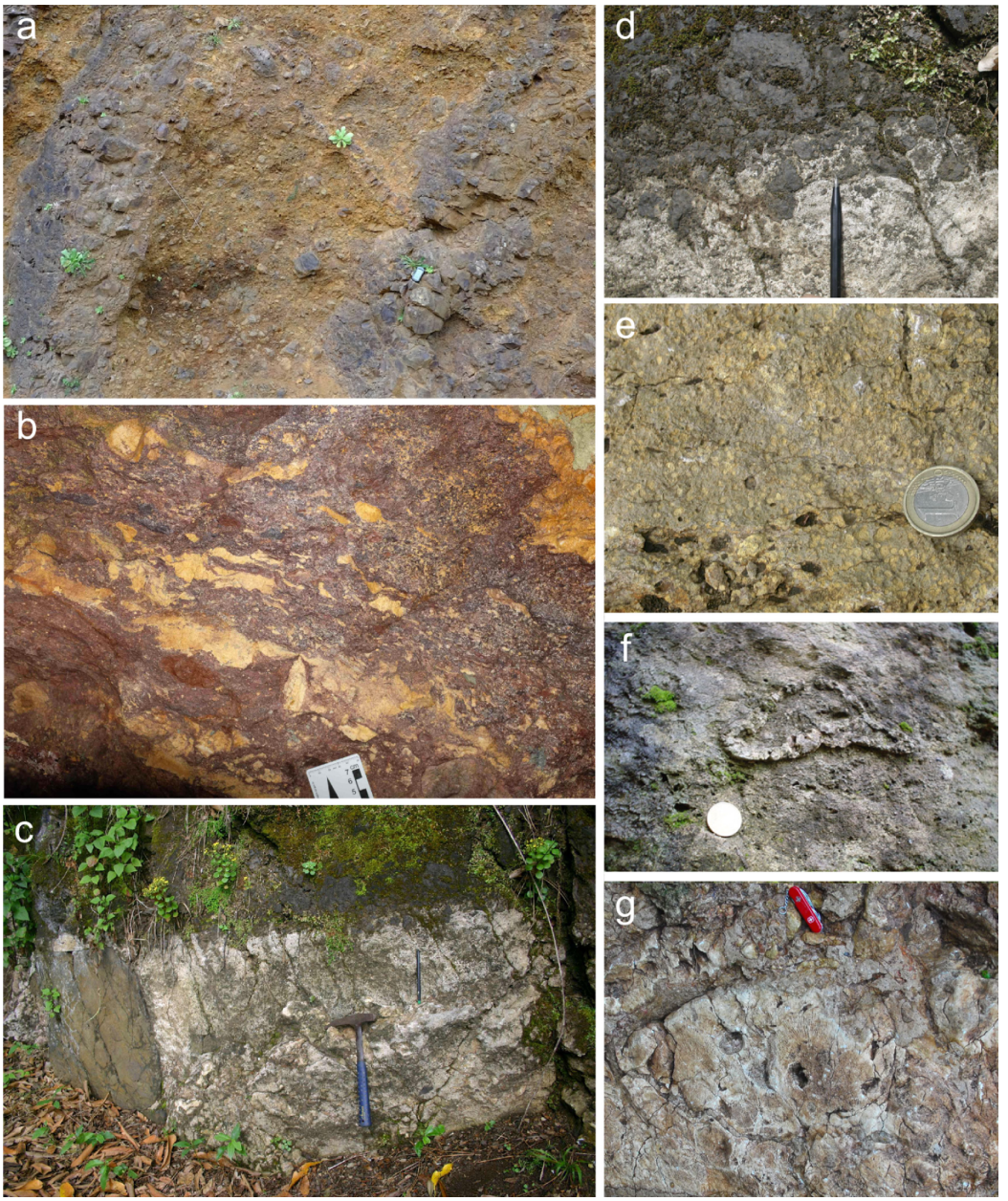

Figure 3. Outcrop photos. (a) Intensely altered pillow and hyaloclastite breccias and penecontemporaneous dykes of CVI1, at Porto da Cruz; (b) blocky and fluidal peperites resulting from the interaction between a pyroclastic flow and the marine sediments; (c) contact between the conglomeratic calcarenites (that terminate the Corgo do Barrinho marine sedimentary sequence) and the overlying subaerial lava flow; (d) detail of contact illustrated on the previous photo; note the blocky peperites that characterize this contact; (e) conglomeratic calcarenites rich in rhodolith debris, from the lower part of the marine sequence; (f) biocalcarenites with large macrofossils. Note the *Clypeaster* sp. test in living position; (g) fossil coral reef structures at the upper part of the sedimentary sequence.

that removed the overlying formations—it is not clear if they are penecontemporaneous with the enveloping CVI1 lithologies or, conversely, coeval with a subsequent magmatic phase.

The upper contact of CVI1 is marked by an erosional unconformity defining a very pronounced topography over which lie the products of the Middle and Upper Volcanic Complexes. The boundary between CVI1 and the sequences of the Middle Volcanic Complex is of particular importance as it reflects the mode of island emergence. Our observations revealed that, throughout the island, where the eroded remains of CVI1 are directly covered by sequences of the Middle Volcanic Complex, the latter are subaerial and dominantly effusive in nature. For example, at Porto da Cruz CVI1 is largely covered by subaerial products of the Encumeada Fm (CVM1), ranging from volcanic and sedimentary breccias to dominantly effusive sequences exposed

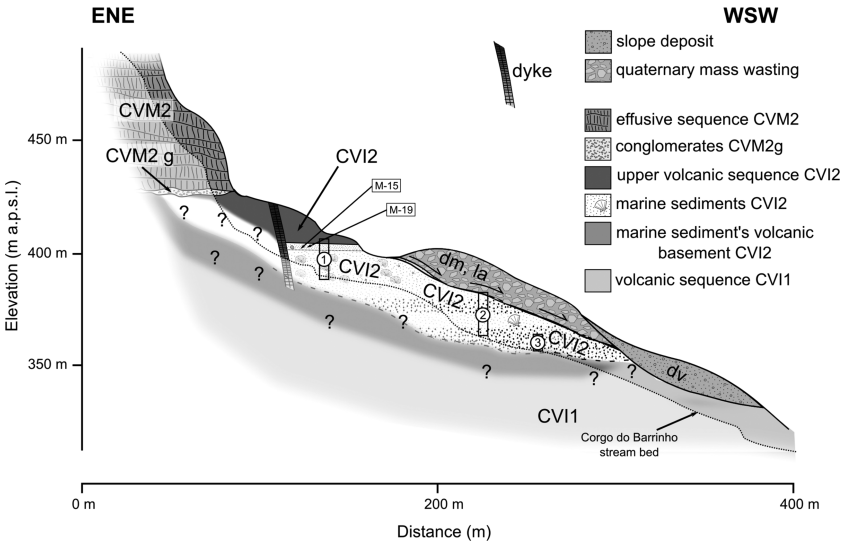

Figure 4. Corgo do Barrinho schematic cross section. Note the approximate position of strip logs at locations with symbols numbered 1, 2, and 3. Approximate position of samples M-15 and M-19 also shown; samples M-05 and M-18 were collected at adjacent Lombo da Eira. (Key: CVI1, Porto da Cruz Fm; CVI2, Lameiros Fm; CVM1, Encumeada Fm; CVM2g, basal conglomerates of Penha D'Águia Fm; CVM2, Penha D'Águia Fm; dv, slope deposits; dm, landslide deposits; la, lahar deposits).

from sea level up to 500 m in elevation. In this same area where the sequences of Encumeada have been eroded away, exposures show that CVI1 was again subsequently mantled (down to present sea level) by lahars and subaerial lava flows of the Penha D'Águia Fm (CVM2), or more recently by products of the Upper Volcanic Complex. Similarly, within São Vicente Valley, exposures at the headwall of the valley and down to 600 m in elevation show that Encumeada subaerial products unconformably overlie the eroded CVI1 edifice (see Figure 2). At lower elevations, CVI1 has been eroded away and the existing topography represents infilling to present sea level by the massive subaerial effusive sequences of Penha D'Águia, a unit that comprises the bulk of the island's shield sequence. More recently, eruptions coeval with the Upper Volcanic Complex extruded subaerial lavas flows that ran down the valley and reached the present-day coastline.

4.2. The Marine Sediments at Sítio dos Lameiros

The marine sediments at Sítio dos Lameiros are wedged between the eroded CVI1 edifice and the effusive sequences of Penha D'Águia (CVM2), the second unit of the Middle Volcanic Complex (see Figure 2). These sediments are exposed along a discontinuous cross section at Corgo do Barrinho canyon, from 360 to 430 m in elevation, in addition to some isolated exposures at the nearby Lombo da Eira (350 m to SW of Corgo do Barrinho) at 320 m in elevation (see Figure 2). The whole area has been exposed by retreat of the valley-bounding vertical cliffs (mostly by mass wasting processes) and is extensively covered by landslide debris and mud and debris flow deposits, a fact that (along with the dense vegetation) contributes to the poor exposure of the in situ sequence. In spite of the poor exposure, at Corgo do Barrinho, it is possible to observe the contact between the marine sediments and overlying basaltic lava flows and pyroclastic flow deposits (see Figures 3b–3d and 4). This contact unambiguously exhibits the presence of blocky peperites, which indicates coeval mixing between rapidly quenched subaerial lava flows and the soft, incoherent sediment that terminates the marine sequence. Along this contact at an old mining cave approximately 50 m SE of this outcrop exposures also exhibit a fluidal peperitic texture, albeit more complex. Here breccias are overlain by purple tuffs. The breccias include highly heterometric (varying from mm-size to dm-size), clasts of compact (and often recrystallized) limestone and basalt, all embedded in a volcaniclastic matrix similar to the overlying tuff. Additionally, irregular pockets of green to grey clay pervasively crosscut the breccias, corresponding to spilitized basaltic injections through the sediment. Despite the complexity of this outcrop, it also reflects magma-sediment interaction, this time with a pyroclastic flow. As such, we can confidently infer that the marine sediments at Lameiros were conformably capped by subaerial volcanic products, noting that CVI2 is in reality a volcano-sedimentary unit. The capping volcanic sequence, however, is not very thick, as the massive effusive succession of Penha D'Águia Fm (and their basal conglomerates) is clearly observable at the valley-bounding cliffs immediately above Corgo do Barrinho, upward of 430–450 m in elevation (Figure 4).

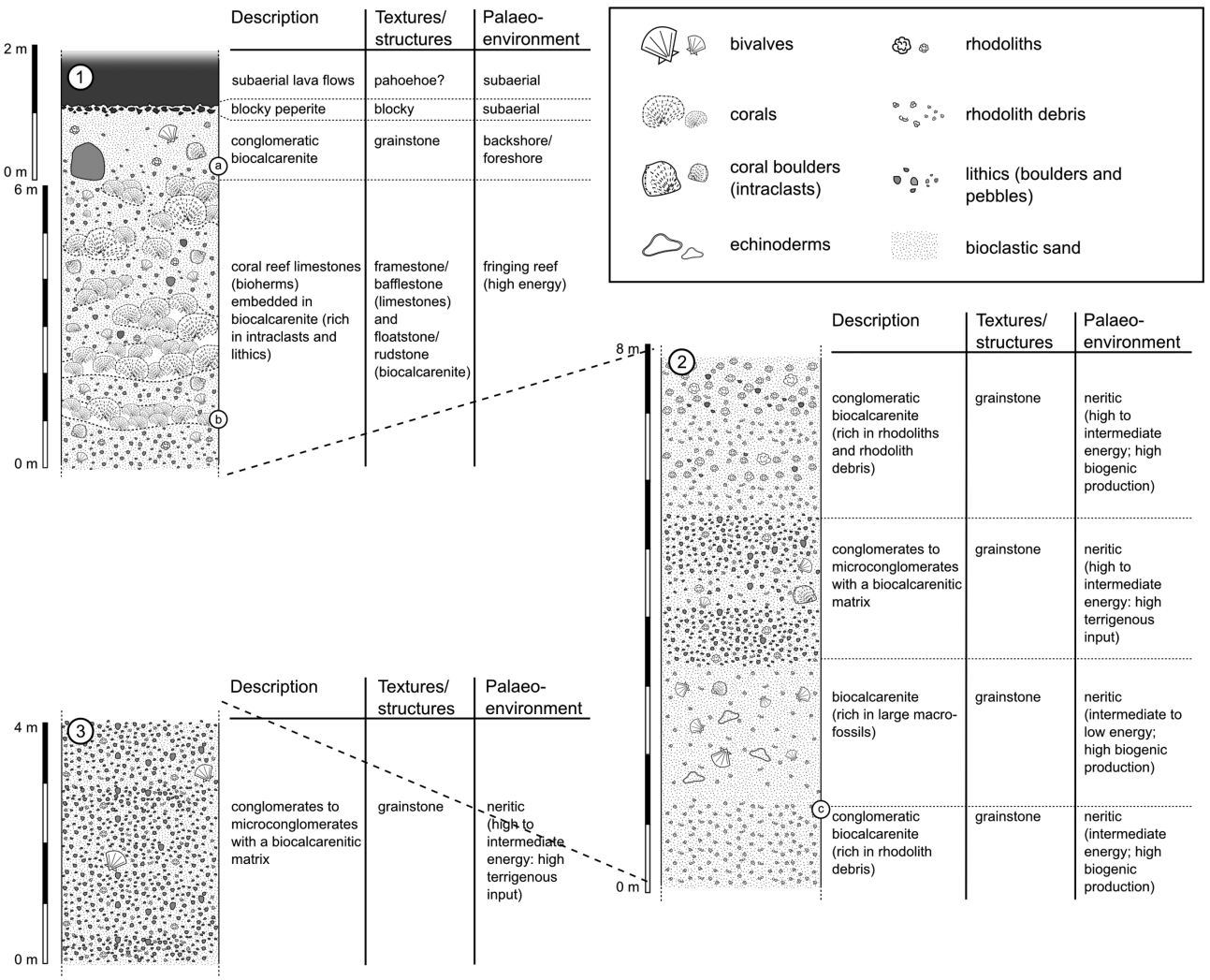

Figure 5. Composite strip logs for marine sediments exposed along Corgo do Barrinho. See Figure 4 for approximate location of individual logs 1, 2, and 3. Letters a, b, and c mark the approximate location of, respectively, the upper, intermediate, and lower sample sets for calcareous nannofossils. Note the transition between submarine and subaerial environments at the top of the sequence.

The contact between the marine sediments and the underlying volcanic lithologies is not exposed at Corgo do Barrinho or Lombo da Eira. The latter, however, are the closest exposures of the underlying volcanic basement, at 310 m in elevation. Our observations reveal that these lithologies must correspond to volcanic products penecontemporaneous with CVI2 (instead of CVI1), as they do not exhibit the same pervasive alteration of typical CVI1 exposures but instead exhibit the same mineral paragenesis rich in plagioclase phenochrysts like the CVI2 peperites. These lithologies constitute the only dateable target stratigraphically below the marine sedimentary sequence and, as such, this site was selected for geochronology (samples M-05 and M-18). Exposures of CVI1 crop out, nevertheless, less than 50 m to the SW and confirm the stratigraphic position of both the sediments and the penecontemporaneous volcanic succession.

4.3. Marine Sediment Characterization and Paleoenvironmental Reconstruction

Despite the discontinuous exposure of the marine limestones at Corgo do Barrinho, it was possible to assemble a composite strip log of the sedimentary sequence (see Figure 5). These sediments generally comprise fossiliferous limestones and biocalcarenites, and conglomerates and microconglomerates with a biocalcarenitic matrix. The following stratigraphic succession was observed, from the base to the top:

1. Conglomerates and microconglomerates with a biocalcarenitic matrix, generally matrix-supported, poorly sorted, with well-rounded pebbles of basaltic nature; abundant rhodolith debris and rare pectinids.

2. Conglomeratic biocalcarenites rich in rhodolith debris and abundant well-rounded pebbles of volcanic nature and broken rhodoliths (Figure 3e); rare large echinoids (mostly complete and incomplete tests of *Clypeaster* sp.), pectinids and other large bivalves; most large shells are disarticulated and many in the stable position.

3. Biocalcarenites with abundant very large macrofossils such as echinoids (mostly tests of *Clypeaster* sp.), coral fragments, pectinids (including the large *Gigantopecten latissimus*), rare oysters and other bivalves, and rare whole rhodoliths. Large shells are all disarticulated and frequently occur in stable positions; echinoid tests are generally complete and in stable positions (Figure 3f).

4. Conglomerates to microconglomerates with a biocalcarenitic matrix, matrix to clast-supported, poorly sorted, rich in rhodolith debris and abundant well-rounded pebbles of volcanic nature and broken rhodolits; rare large echinoids (tests), pectinids and other large bivalves frequently in the stable position; rare boulders of coral (intraclasts).

5. Conglomeratic biocalcarenite, with irregular alternating layers rich in rhodoliths (typically smaller than 1 cm but occasionally 1–3 cm) and rhodolith debris; rare large pectinids and other bivalves.

6. Reefal limestones (Figure 3g), dominated by coral bioedifications—bioherms—embedded in biocalcarenites with abundant coral fragments, pectinids, rare oysters and fragments of other shelly mollusks; bioherms range from small (30–50 cm) coral piles to irregular and dome-shaped masses usually less than $\sim$1 m in diameter and in height (Figure 3g).

7. Conglomeratic calcarenites with abundant well-rounded volcanic clasts, of variable size, and containing echinoid spicules, coral boulders (bioeroded), rare pectinids and oysters, and fragments of other shelly mollusks.

8. Peperites (Figures 3b–3d) and mafic lava and pyroclastic flows.

The results of our calcareous nannofossil screening are summarized in Table 2. Preservation of the fossil assemblages are poor and often have etched or recrystalized rims. However, this taphonomic effect does not introduce important bias due to strong diagenetic lixiviation and elimination of important components of the assemblage because small (<3 μm) specimens are still present. Concerning their biostratigraphy, the overall assemblages are compatible with an upper Miocene-lower Pliocene age interval (Tortonian-Zanclean), despite the absence of classic biostratigraphic markers (e.g., species of discoasterids [see *Bown*, 1998]). Finally, in terms of paleoenvironment, featured associations are relatively diverse indicating open marine conditions. However, specimens belong to placolith robust taxa with scarce presence of typical deep ocean genera such as the *Sphenolithus* and *Discoaster*, perhaps a reflection of deposition in a shelf environment. The associations found across the entire sedimentary sequence at Corgo do Barrinho are compatible with those found in similar Miocene to Pliocene coastal transitions from submarine to subaerial volcanic sequences on other volcanic islands such as Porto Santo (Madeira Archipelago) [*Cachão et al*., 1998], Santiago and São Nicolau from Cape Verde Archipelago [*Johnson et al*., 2012, 2014].

The sedimentary sequence at Corgo do Barrinho preserves a faint but discernible subhorizontal (or dipping gently to the north) stratification, with a vertical facies variation between more energetic and lithic-rich conglomeratic lithologies to biocalcarenites, and then to coral reef limestones and beach biocalcarenitic deposits. No obvious lateral variations were observed. The sequence replicates a general fining-upward pattern (despite some rhythmic fining and coarsening in the middle of the sequence) with decreasing terrigenous input and increasing biogenic contribution toward the top. The section generally corresponds to the onlap of marine sediments against a steep rocky shore and offshore slope, carved on the emerged portion of the volcanic edifice, and reflects the gradual development of a small fringing coral reef (typical of very young volcanic coastlines in warm seas) and overlying perched sandy beach. The sequence also suggests a progressive transgression until the stabilization of a coastal marine paleoenvironment before it was capped abruptly by subaerial volcanic deposits. Finally, the fossiliferous content suggests a paleoenvironment typical of oceanic tropical to subtropical (warm) waters, similar to other Miocene outcrops in nearby Porto Santo [*Johnson et al*., 2011; *Santos et al*., 2011, 2012; *Mata et al*., 2013] and other Atlantic islands [e.g., *Serralheiro*, 1976; *Ávila et al*., 2012; *Johnson et al*., 2014].

4.4. $^{40}Ar/^{39}Ar$ Geochronology

The $^{40}Ar/^{39}Ar$ data for samples corresponding to the sediment's volcanic basement are presented as incremental age spectra in Figure 6. Isochron plots from the $^{40}Ar/^{39}Ar$ data are not presented here because no

Table 2. List of Calcareous Nannofossils Found at Corgo do Barrinho, for Each Sample Subset

Lower Sample Set	Intermediate Sample Set	Upper Sample Set
Cyclicargolithus floridanus	*C. pelagicus* s.l.	*C. pelagicus* s.l.
Coccolithus pelagicus s.l.	*D. antarticus*	*Calcidiscus leptoporus*
Dictyococcites antarticus	*Dictyococcites productus* (<3 μm)	*D. productus*
(=*Reticulofenestra antarticus*)	(=*Reticulofenestra productus*)	*D. antarticus*
Discoaster sp. (six arms, recristalyzed)	Small *Gephyrocapsa* spp. (<3 μm)	Small *Gephyrocapsa* spp. (<3 μm)
Helicosphaera carteri	*R. haqii-minutula*	*H. carteri*
Small *Gephyrocapsa* spp. (<3 μm)	*Reticulofenestra minuta* (<3 μm)	*P. lacunosa* (?)
Pseudoemiliania lacunosa (?)		*R. haqii-minutula*
Reticulofenestra haqii-minutula (3–7 μm)		*R. minuta*
Reticulofenestra pseudoumbilicus		*Sphenolithus* sp.
Sphenolithus abies-neoabies		

statistically meaningful regressions can be made through the individual data points. Given the criteria in this study used for determining an $^{40}Ar/^{39}Ar$ plateau age (>50% of the cumulative ^{39}Ar gas released in three or more contiguous heating steps with statistically identical ages at the 2σ level of uncertainty), the volcanic basement basalt M-05 is the only sample that satisfied those criteria yielding an $^{40}Ar/^{39}Ar$ plateau age of 6.86 $\pm$ 0.07. Other $^{40}Ar/^{39}Ar$ results, particularly those from basalt boulders within the marine sediments (CV12) are less precise, but of similar overall age and we make preferred inferences as to their eruption ages by weighting selected contiguous $^{40}Ar/^{39}Ar$ incremental steps with high radiogenic argon concentrations and similar ages. For example, data from sample M-18, although they plot as a relatively flat $^{40}Ar/^{39}Ar$ age spectrum, no $^{40}Ar/^{39}Ar$ plateau age can be calculated with the strict criteria mentioned above. However, a weighted mean $^{40}Ar/^{39}Ar$ age determined from the last five incremental heating steps that also have the highest radiogenic argon ($^{40}Ar*$) contents results in a preferred $^{40}Ar/^{39}Ar$ age of 6.5 $\pm$ 0.4 Ma (2σ). Samples M-15 and M-19, from clasts within the marine sediments, have similar $^{40}Ar/^{39}Ar$ age spectra, with old and progressively decreasing apparent ages in the low to midtemperature heating steps and relatively constant but younger ages in the highest temperature heating steps. The $^{40}Ar/^{39}Ar$ age spectra from these two samples are consistent with the presence of excess argon, possibly related to alteration of the basalt. However, weighted mean ages of the high-temperature steps for samples M-15 and M-19, which also have the highest $^{40}Ar*$ contents, yield preferred ages of 7.0 $\pm$ 0.8 and 6.7 $\pm$ 0.4 Ma, respectively. Collectively, the $^{40}Ar/^{39}Ar$ data from all of the basalt samples indicate a narrow age range (6.5–7.0 Ma) for the underlying volcanic sequence, with the most precisely dated sample (M-05) at 6.86 $\pm$ 0.07 Ma.

5. Discussion

The oldest geological unit of Porto da Cruz Fm (CVI1) exhibits characteristics of a subaqueous volcanic nature, dominantly clastic and autoclastic, and more rarely effusive. This submarine origin is consistent with the presence of structures/textures that correspond to hyaloclastites and pillow breccias, and also by a pervasive palagonitic alteration as confirmed by XRD data. As such, CVI1 represents the remnants of a volcanic seamount building phase, similar to other very similar basal units found across the Atlantic islands—e.g., La Palma, Porto Santo, São Nicolau, Santiago, and Brava [*Staudigel and Schmincke*, 1984; *Schmidt and Schmincke*, 2002; *Macedo et al*., 1988; *Serralheiro*, 1976; *Madeira et al*., 2010; *Ramalho*, 2011].

Present-day exposures of CVI1 are confined to two areas along the northern half of the island, where they can be found up to ~800 m in elevation. These elevations, together with the steep erosive unconformity that truncates this unit, signifies that the volcanic edifice exhibited a prominent but irregular paleotopography before it was covered by subsequent stratigraphic units. More importantly, this means that the submarine edifice was gradually exposed to subaerial erosion by a relative fall of sea level prior to being covered by subsequent subaerial shield volcanism. Thus, the geological record of Madeira Island unequivocally shows that, in the long run, island emergence essentially took place by a relative sea-level fall and not by summit volcanism. Indeed, even if surtseyan volcanism occurred during edifice shoaling and its products were subsequently eroded, it must have played a minor role during the process of emergence.

Unfortunately, no outcrops of CVI1 were found with lithologies pristine enough for dating. Despite this limitation—and assuming a Late Miocene age for CVI1—a minimum vertical displacement of ~750 m is required to raise the top of CVI1 above coeval sea-level highstands (reaching a maximum of ~50 m above

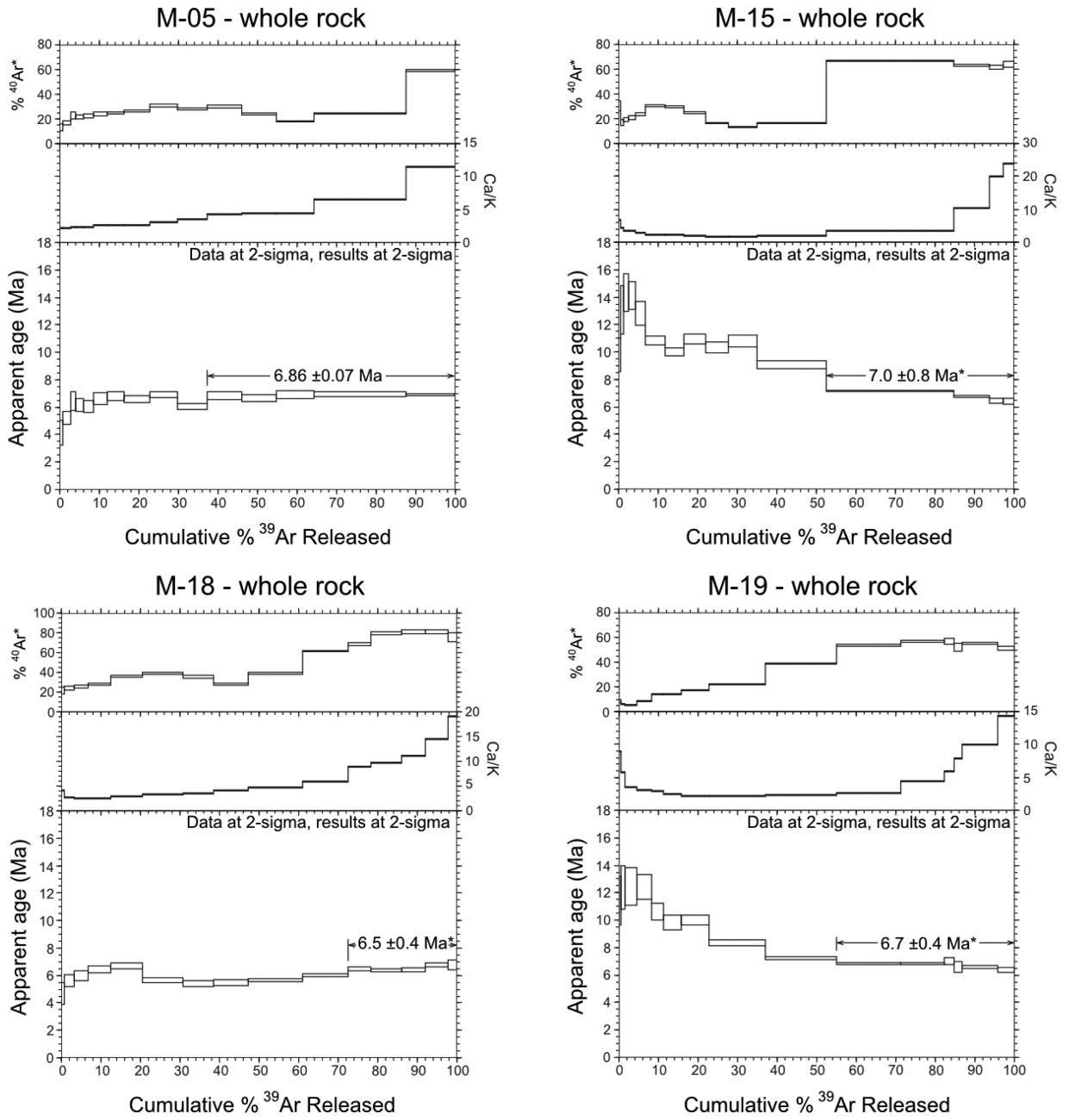

Figure 6. $^{40}Ar/^{39}Ar$ age spectra of selected samples from CO_2-laser incremental heating experiments. Each $^{40}Ar/^{39}Ar$ age spectrum plots the cumulative $\%^{39}Ar$ released per heating step versus apparent age (Ma), Ca/K ratio, and radiogenic argon ($^{40}Ar*$). Sample M-05 yielded an $^{40}Ar/^{39}Ar$ plateau age ($\geq$ 3 contiguous heating steps comprising $\geq$ 50% of cumulative ^{39}Ar released with ages overlapping at the 2σ level of uncertainty) of 6.86 $\pm$ 0.07 Ma. Samples M-15, M-18, and M-19 failed to yield plateau ages, and for these samples, we calculated weighted mean ages for incremental heating steps toward the end of the experiments (identified by asterisks) that had nearly similar ages and high radiogenic argon contents. The resulting ages are less precise (7.0 $\pm$ 0.8 Ma, 6.5 $\pm$ 0.4 Ma, and 6.7 $\pm$ 0.4 Ma, respectively) but are sufficient to show that these basalts were erupted in a narrow time interval between about 6.5 and 7 Ma. All reported ages (results) and the heights of boxes for individual heating steps (data) are shown with 2σ levels of uncertainty.

present sea level (a.p.s.l.)) [see *Miller et al*., 2005] to its present elevation, indicating that the submarine edifice inevitably experienced substantial uplift. Therefore, we can infer that the emergence of Madeira Island is essentially due to uplift, which occurred before volcanism resumed to form the bulk of the voluminous subaerial shield volcano we see today.

The presence of marine sediments at Corgo do Barrinho offers a unique opportunity to understand the timing and mode of emergence of Madeira's edifice. These outcrops are essentially wedged between CVI1 and the bulk of the Middle Volcanic Complex and record the significant vertical movements that affected Madeira's

early evolutionary history, as pointed out by previous authors [e.g., *Mata et al*., 1995; *Mata*, 1996; *Mata et al*., 2013]. Our paleoenvironmental reconstructions suggest that the marine sedimentary sequence at Corgo do Barrinho essentially corresponds to the establishment of a tropical to subtropical shoreline, with onlap and development of a small fringing coral reef and adjacent perched beach against a steep rocky shore during the late Miocene. Furthermore, the outcrops at Corgo do Barrinho (despite the poor exposure) clearly document the transition between submarine and subaerial environments (Figure 5), marking very accurately sea level when sedimentation was abruptly interrupted by subaerial volcanic activity. This transition is presently at 430 m a.p.s.l. and the presence of peperites at the transition zone provides unequivocal evidence that the overlying volcanic sequence is penecontemporaneous with the underlying sediments. This study clearly demonstrates that the Lameiros stratigraphic unit (CVI2) is not exclusively composed of marine sediments, but also includes penecontemporaneous volcanic formations that should be the focus of further research.

The precise age of the marine sequence at Corgo do Barrinho has proven difficult to date. It was initially considered as "Vindobonian" (15.5–11.0 Ma) on the basis of its macrofauna [*Romariz*, 1971a, 1971b; *Mitchell-Thomé*, 1974; *Zbyszewski et al*., 1975], using criteria that are now considered invalid [*Mata et al*., 2013]. Later, *Ferreira et al*. [1988] considered it to be younger than 5.2 Ma, based on a K-Ar age on a seemingly subjacent lava flow. *Ramalho* [2011] attempted dating the sediments using strontium isotope stratigraphy on macrofossils extracted from the sedimentary sequence. Four fossils were analyzed and yielded an age between 9 and 10 Ma; however, high values of Fe and Mn suggest that the fossils were not pristine enough to yield an accurate numerical age. In order to get a more precise age constraint on these sediments, in this study, we used $^{40}Ar/^{39}Ar$ geochronology of underlying volcanic rocks and boulders included within the sedimentary sequence to provide maximum age constraints on the sediments. Our data indicate a narrow time interval (6.5–7.0 Ma) for the eruption of these volcanic rocks, which is in general agreement with calcareous nannofossil biostratigraphy and provides an approximate age for the consolidation of the sediments. Additionally, these results show unequivocally that subaerial volcanism at Madeira Island started at least 1.4 Myr earlier than previously reported, allowing a refinement of existing hotspot track models [e.g., *Geldmacher et al*., 2005].

The $^{40}Ar/^{39}Ar$ geochronology results presented here constrain the age of the coastline preserved at Corgo do Barrinho to 6.5–7.0 Ma, and therefore provide a vertical benchmark that we can use to estimate the amount of uplift experienced by Madeira Island during its initial stages of island building. Effectively, the establishment of such coastline at ~6.9 Ma and subsequent uplift to its present elevation at 430 m—before the onset of subaerial shield volcanism no later than ~5.6 Myr ago [*Ech-chakrouni*, 2004]—requires a minimum vertical displacement on the order of ~405 m in ≤1.4 Myr (assuming that the highest estimated sea-level highstand during the considered time interval corresponds to ~25 m a.p.s.l. [*Miller et al*., 2005]). This corresponds to a minimum uplift rate of ~290 m/Myr, a relatively high value for the Atlantic context. As a comparison, Santiago, São Nicolau, and Brava (Cape Verde) experienced uplift rates of 97, ~32, and ~210 m/Myr, respectively, whereas La Palma in the Canary Islands experienced higher uplift rates of 400–600 m/Myr [*Ramalho*, 2010; *Ramalho et al*., 2010a; *Madeira et al*., 2010; *Klügel et al*., 2005].

The evidence presented here therefore suggests that Madeira Island edifice (a seamount) emerged essentially by an uplift process, possibly without involving summit surtseyan volcanism. Because it was not possible to date CVI1 directly, the maximum elevation at which this unit crops out (800 m a.p.s.l., 370 m above Corgo do Barrinho benchmark) cannot be used to compute a longer-term uplift rate. Nonetheless, this fact indicates that the amount of uplift was much higher than that recorded by the marine limestones, and that the uplifting process started earlier than the establishment of a paleo-shore at Corgo do Barrinho, showing that the emergence of a large volcano is a protracted process. The $^{40}Ar/^{39}Ar$ ages reported here represent the best current time estimate for the emergence of the Madeira Island edifice.

The geological record at vertically stable or uplifting volcanic oceanic islands is almost invariably rich with geologic evidence for higher relative sea level, such as submarine volcanic products, marine terraces, and wave-cut notches [e.g., *Zazo et al*., 2007; *Madeira et al*., 2010; *Ramalho*, 2011; *Ramalho et al*., 2013] that were formed during recurring glacio-eustatic highstands higher than present sea level [*Miller et al*., 2005; *Bintanja et al*., 2005] and preserved within the now subaerially exposed coastal sequences/morphology. However, our study confirms that the Middle and Upper Volcanic Complexes of Madeira Island are entirely subaerial in nature, with the notable exception of a few very recent hydromagmatic explosive products associated with coastal eruptions. Furthermore, even on old stretches of coast sheltered from rapid marine erosion (e.g., on the southeastern coast of the island), no morphological or stratigraphic evidence can be found for recent

highstands such as Marine Isotope Stages 5e, 7 or 11, as observed on uplifting or vertically stable island edifices (e.g., Santa Maria in the Azores, Sal, Santiago, and São Nicolau in the Cape Verdes). For these reasons, we infer that Madeira Island probably entered a slow process of subsidence during subaerial shield volcanism.

In summary, we infer that Madeira Island emerged through an uplift process rather than volcanic activity around 7.0–5.6 Ma, and probably slowly subsided ever since. The origins of this complex uplift/subsidence trend are not yet completely understood and need further research. Presently, it is not possible to correlate the timing of uplift episodes at Madeira and Porto Santo but these two islands may have experienced coeval uplift. If the latter is true, it could be interpreted as a sign of regional uplift driven by buoyancy changes in the mantle beneath these islands. However, the contrasting maximum uplift magnitudes between Madeira and Porto Santo (750 versus 365 m, respectively) on such small spatial scales (the islands are only ~40 km apart) suggests a local rather than regional uplift source—possibly driven by basal intrusions—as it has been inferred for other Atlantic islands [*Staudigel and Schmincke*, 1984; *Klügel et al*., 2005; *Ramalho*, 2010; *Ramalho et al*., 2010a, 2010b; *Madeira et al*., 2010]. Similarly, we infer that the syn-subaerial shield subsidence trend at Madeira may be linked to flexural surface loading associated with the vigorous volcanism that formed the bulk of the island's subaerial edifice.

There are several implications of this study. First, it confirms that islands may emerge through a slower uplift process rather than the relatively fast process of summit volcanism, which necessarily implies very high magma supply rates. Thus, even seamounts subjected to very low summit eruption rates may still breach the sea surface and become islands, but only if they experience enough uplift. When they shoal, submarine volcanic edifices with low summit eruption rates do not grow fast enough to compensate for marine erosion and so rarely become islands—unless slow volcanic growth is compensated by uplift [*Ramalho et al*., 2013]. This type of emergence involving uplift and volcanic quiescence has been reported in many other islands located on the slow-moving Nubian plate, e.g., La Palma, Sal, Maio, Santiago, São Nicolau, and Brava [*Staudigel and Schmincke*, 1984; *Klügel et al*., 2005; *Ramalho*, 2010; *Ramalho et al*., 2010a, 2010b; *Madeira et al*., 2010]. Brava, for example, represents a former seamount (no older than 3 Ma) that uplifted about 300 m during a volcanic gap lasting about 1.3 Myr until 0.25 Ma, and continued to uplift an extra 100 m into the Holocene [*Madeira et al*., 2010]. This perhaps suggests that plate-movement exerts an indirect influence on the mode of island emergence. In slow moving to stationary plates with respect to existing sources of partial melting (i.e., hot spots), magmatism is inevitably more concentrated in space and time leading to longer but more intermittent island magmatic histories and higher degrees of crustal thickening driven by intrusive processes (the main source of uplift). Therefore, in these settings, chances for emergence by uplift between eruptive periods are thus increased, in contrast to fast-moving plate settings such as in the Pacific Ocean [*Ramalho et al*., 2013]. More importantly, given the aforementioned considerations, the geological record in these islands possibly shows that uplift and subsidence in oceanic islands is essentially governed by competing processes of internal growth (intrusions) and surface loading (volcanism). In other words, we propose that island edifice growth may reflect an alternation between dominantly volcanic and dominantly intrusive activity. Finally, Madeira's Archipelago complex uplift/subsidence history also serves to highlight that our knowledge on island isostasy and its relation to volcanism/plutonism is, perhaps, still in its infancy.

6. Summary and Conclusions

Our study on the mode and timing of emergence of Madeira Island reveals that the bulk of Madeira's subaerial shield edifice lies unconformably over the eroded remains of a volcanic seamount that was exposed subaerially prior to the extrusion of the subaerial shield sequence. The marine sediments at Sítio dos Lameiros, within São Vicente Valley, constitute a solid benchmark that helps constrain the history of vertical movements affecting Madeira Island, and their present position at 320–430 m a.p.s.l. has now been largely reconciled with the island's stratigraphy. These observations suggest that Madeira Island's proto-edifice emerged above sea level essentially by means of uplift and not summit volcanism between 5.6 and 7.0 Ma ago, and involving over 405–750 m of vertical displacement. The source of such uplift is probably related to basal intrusions, as it has been inferred for other islands located in the Nubian plate.

Several implications may be drawn from this study concerning ocean island evolution on slow-moving vs fast-moving plate settings, with respect to melting source behind island volcanism. First, this study shows that island emergence, i.e. the transition between seamount and emerged island, may take place by means of a

relative fall of sea level through uplift, eustatic changes or a combination of both, and may not involve significant summit surtseyan volcanism. This mechanism is more likely to occur on island edifices subjected to long but intermittent magmatic lives and uplift trends, such as the ones located on slow-moving to stationary plates with respect to their melting source. Finally, the complex vertical movement history experienced by many islands in the Nubian plate - with alternating uplift and subsidence episodes - suggests that island edifice growth may be governed by competing dominantly volcanic and dominantly intrusive processes.

Appendix A: XRD Diffractograms

X-ray diffraction of two samples from Porto da Cruz Formation were performed to confirm palagonitization of its volcanic products. Figure A1 presents the diffractograms of one sample from the basal submarine unit (PC-02) and another one of a subaerial lava (M-21) for comparison. The second sample from Porto da Cruz Formation (PC-01) yielded a similar diffractogram.

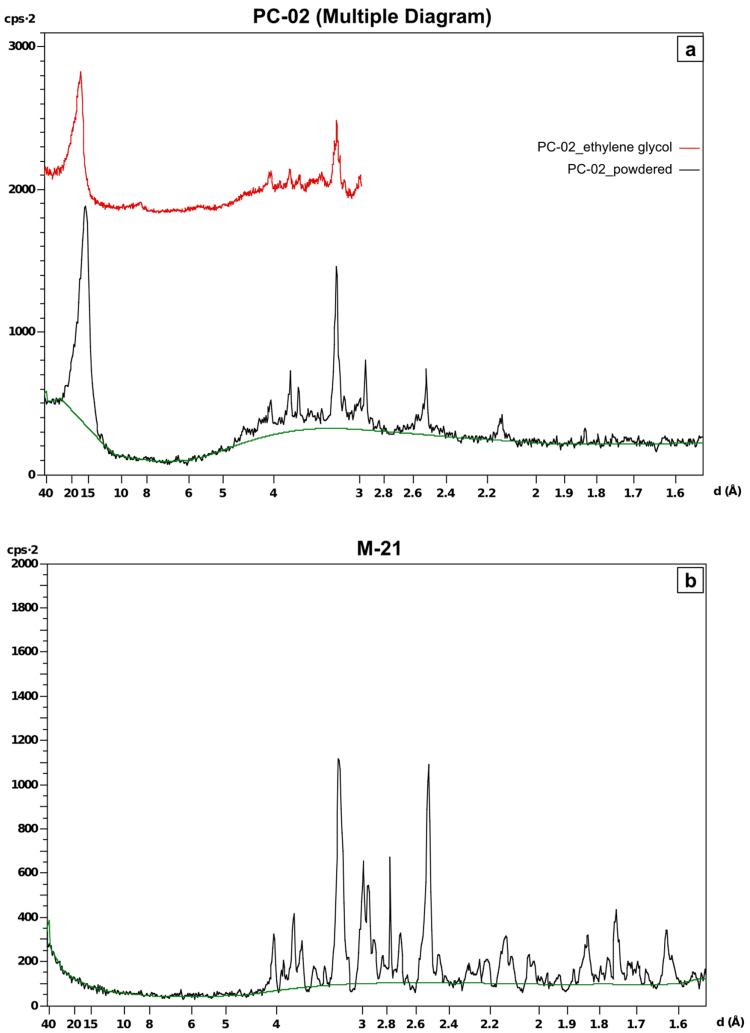

Figure A1. XRD diffractograms for samples PC-02 and M-21 (sample PC-01 is virtually identical to PC-02). (a) X-ray-diffraction patterns (CuKα radiation) for the powdered sample PC-02 (Porto da Cruz palagonitized basalt) and X-ray diffraction traces of oriented aggregates solvated with ethylene glycol (in red). Note the numerous mineral peaks arising from a hump (in green). The hump derives from the presence of glass to amorphous material in the sample, and these overall characteristics are typical of samples from rocks that experienced a palagonitization process as a result of seawater/basalt interaction [see *Gurenko and Schmincke*, 1998; *Stroncik and Schmincke*, 2002; *Achilles et al.*, 2013]. (b) XRD patterns of the bulk-rock powdered sample PC-02 (Porto da Cruz palagonitized basalt) oriented aggregate. Several peak minerals like saponite (a trioctahedral smectite 15.78 and 4.53 Å), maghemite (2.51 and 1.47 Å), and hematite, phillipsite (a hydrated potassium, calcium, and aluminum zeolite 2.93 Å), opale (4.08 and 2.51 Å), apatite (2.69 and 2.79 Å), anhydrite (3.50 and 2.85 Å), and tridymite (4.26, 4.07, and 3.80 Å), among others, emerge from a hump of vitreous/amorphous material (in green) [see *Stroncik and Schmincke*, 2002; *Michalski et al.*, 2005; *Achilles et al.*, 2013]. (c) Bulk XRD spectra (CuKα radiation) of M-21, a control sample of subaerial basalt from the Cabo Girão effusive succession, showing the typical mineral peaks of basalt.

Acknowledgments

Data supporting Figure 6 are available as supporting information data set 1. The old quarry and lime kilns at Lameiros have been preserved and integrated in a Museum Centre by the initiative of Rota da Cal—Associação de Investigação e Divulgação de Fornos de Cal, a private NGO, to whom we acknowledge and commend for their work in preserving this geological and cultural heritage. The $^{40}Ar/^{39}Ar$ Geochronology presented in this paper was partially funded by Rota da Cal, within their musealization initiative cofunded by PRODERAM (Secretaria Regional do Ambiente e Recursos Naturais) under the European Agricultural Fund for Rural Development (EAFRD/FEADER). R. Ramalho was funded by an FP7-PEOPLE-2011-IOF Marie Curie Postdoctoral Fellowship, which is gratefully acknowledged. A.B.S., P.E.F., J.M. and M.C. acknowledge FCT funding trough Project LA-0019 IDL. We thank T. Becken (Editor), A. Klügel, K. Turner, and an anonymous reviewer for their very helpful comments. Any use of trade, product, or firm names is for descriptive purposes only and does not imply endorsement by the U.S. Government.

References

Achilles, C. N., R. V. Morris, S. J. Chipera, D. W. Ming, and E. B. Rampe (2013), X-ray diffraction reference intensity ratios of amorphous and poorly crystalline phases: Implications for CHEMIN on the Mars Science Laboratory Mission, *Proc. Lunar Planet. Sci. Conf.*, 44th, 3072.

Ávila, S. P., R. Ramalho, and R. Vullo (2012), Systematics, palaeoecology and palaeobiogeography of the Neogene fossil sharks from the Azores (Northeast Atlantic), *Ann. Paléontol.*, *98*(3), 167–189.

Bintanja, R., R. S. van de Wal, and J. Oerlemans (2005), Modelled atmospheric temperatures and global sea levels over the past million years, *Nature*, *437*(7055), 125–128.

Bonatti, E. (1965), Palagonite, hyaloclastites and alteration of volcanic glass in the ocean, *Bull. Volcanol.*, *28*(1), 257–269.

Bown, P. (1998), *Calcareous Nannofossil Biostratigraphy, Br. Micropalaeontol. Soc. Publ. Ser.*, Chapman and Hall, London.

Brum da Silveira, A., J. Madeira, R. Ramalho, P. Fonseca, C. Rodrigues, and S. Prada (2010a), Carta Geológica da Ilha da Madeira na escala de 1:50000, Folha A, technical report, Secr. Reg. do Ambiente e Recursos Naturais, Governo Reg. da Madeira, Funchal, Madeira Island.

Brum da Silveira, A., J. Madeira, R. Ramalho, P. Fonseca, C. Rodrigues, and S. Prada (2010b), Carta Geológica da Ilha da Madeira na escala de 1:50000, Folha B, technical report, Secr. Reg. do Ambiente e Recursos Naturais, Governo Reg. da Madeira, Funchal, Madeira Island.

Brum da Silveira, A., J. Madeira, R. Ramalho, P. Fonseca, C. Rodrigues, and S. Prada (2010c), Notícia Explicativa da Carta Geológica da Ilha da Madeira na escala de 1:50000, technical report, Secr. Reg. do Ambiente e Recursos Naturais, Governo Reg. da Madeira, Funchal, Madeira Island.

Cachão, M., D. Rodrigues, C. M. da Silva, and J. Mata (1998), Biostratigrafia (Nanofósseis calcários) e interpretação paleoambiental do Neogénico de Porto Santo (Madeira), Dados preliminares, *Comun. Inst. Geol. Mineiro*, *84*, A185–A188.

Ech-chakrouni, S. (2004), Géochronologie et Paléomagnetisme de lîle de Madère et des îles Desertas: Une contribution à la volcanostratigraphie et à l'évolution de l'árchipel de Madère et á l'échelle de polarité du champ géomagnétique, PhD thesis, Vrije Univ, Brussels, Belgium.

Feraud, G., J. Gastaud, H. Schmincke, G. Pritchard, J. Lietz, and U. Bleil (1981), New K-Ar ages, chemical analyses and magnetic data of rocks from the islands of Santa Maria (Azores), Porto Santo and Madeira (Madeira Archipelago) and Gran Canaria (Canary Islands), *Bull. Volcanol.*, *44*(3), 359–375.

Ferreira, M., C. Macedo, and J. Ferreira (1988), K-Ar geochronology in the Selvagens, Porto Santo and Madeira islands (Eastern Central Atlantic): A 30 m.y. spectrum of submarine and subaerial volcanism, *Lunar Planet. Sci. Conf. Abstr.*, *19*, 325.

Ferreira, M. P. (1985), Evolução geocronológica e paleomagnética das ilhas do arquipélago da Madeira—Uma síntese, *Mem. Not. Univ. Coimbra*, *99*, 213–218.

Furnes, H. (1984), Chemical changes during progressive subaerial palagonitization of a subglacial olivine tholeiite hyaloclastite: A microprobe study, *Chem. Geol.*, *43*(3), 271–285.

Geldmacher, J., and K. Hoernle (2000), The 72 Ma geochemical evolution of the Madeira hotspot (eastern North Atlantic): Recycling of Paleozoic ($\leq$500 Ma) oceanic lithosphere, *Earth Planet. Sci. Lett.*, *183*(1–2), 73–92.

Geldmacher, J., P. van den Bogaard, K. Hoernle, and H. Schmincke (2000), The $^{40}Ar/^{39}Ar$ age dating of the Madeira Archipelago and hotspot track (eastern North Atlantic), *Geochem. Geophys. Geosyst.*, *1*(2), 1008, doi:10.1029/1999GC000018.

Geldmacher, J., K. Hoernle, P. Bogaard, S. Duggen, and R. Werner (2005), New $^{40}Ar/^{39}Ar$ age and geochemical data from seamounts in the Canary and Madeira volcanic provinces: Support for the mantle plume hypothesis, *Earth Planet. Sci. Lett.*, *237*(1–2), 85–101.

Gurenko, A. A., and H.-U. Schmincke (1998), Geochemistry of sideromelane and felsic glass shards in Pleistocene ash layers at sites 953, 954, and 956, in *Proceedings of Ocean Drilling Program, Scientific Results*, vol. 157, edited by P. Weaver et al., pp. 421–428, Ocean Drill. Program, College Station, Tex.

Johnson, M., B. Baarli, M. Cachão, C. da Silva, J. Ledesma-Vázquez, E. Mayoral, R. Ramalho, and A. Santos (2012), Rhodoliths, uniformitarianism, and Darwin: Pleistocene and recent carbonate deposits in the Cape Verde and Canary archipelagos, *Palaeogeogr. Palaeoclimatol. Palaeoecol.*, *329–330*, 83–100.

Johnson, M. E., C. M. da Silva, A. Santos, B. G. Baarli, M. Cachão, E. J. Mayoral, A. C. Rebelo, and J. Ledesma-Vázquez (2011), Rhodolith transport and immobilization on a volcanically active rocky shore: Middle Miocene at Cabeço das Laranjas on Ilhéu de Cima (Madeira Archipelago, Portugal), *Palaeogeogr. Palaeoclimatol. Palaeoecol.*, *300*(1), 113–127.

Johnson, M. E., R. S. Ramalho, B. G. Baarli, M. C. Ao, C. M. da Silva, E. J. Mayoral, and A. Santos (2014), Miocene-pliocene rocky shores on são nicolau (Cape Verde islands): Contrasting windward and leeward biofacies on a volcanically active oceanic island, *Palaeogeogr. Palaeoclimatol. Palaeoecol.*, *395*, 131–143, doi:10.1016/j.palaeo.2013.12.028.

Klügel, A., T. Hansteen, and K. Galipp (2005), Magma storage and underplating beneath Cumbre Vieja volcano, La Palma (Canary Islands), *Earth Planet. Sci. Lett.*, *236*(1–2), 211–226.

Klügel, A., S. Schwarz, P. van den Bogaard, K. Hoernle, C. Wohlgemuth-Ueberwasser, and J. Köster (2009), Structure and evolution of the volcanic rift zone at Ponta de São Lourenço, eastern Madeira, *Bull. Volcanol.*, *71*(6), 671–685.

Kokelaar, B. (1983), The mechanism of Surtseyan volcanism, *J. Geol. Soc.*, *140*(6), 939–944.

Kokelaar, B. (1986), Magma-water interactions in subaqueous and emergent basaltic, *Bull. Volcanol.*, *48*(5), 275–289.

Kuiper, K., A. Deino, F. Hilgen, W. Krijgsman, P. Renne, and J. Wijbrans (2008), Synchronizing rock clocks of Earth history, *Science*, *320*(5875), 500–504.

Lee, J.-Y., K. Marti, J. P. Severinghaus, K. Kawamura, H.-S. Yoo, J. B. Lee, and J. S. Kim (2006), A redetermination of the isotopic abundances of atmospheric Ar, *Geochim. Cosmochim. Acta*, *70*(17), 4507–4512.

Macedo, J., A. Serralheiro, and L. Silva (1988), Notícia Explicativa da Carta Geológica da Ilha de S. Nicolau (Cabo Verde) na escala de 1: 50000, *Garcia Orta Serv. Geol.*, *11*(1–2), 1–32.

Machado, F. (1962), Sobre o mecanismo da erupção dos Capelinhos, *Mem. Serv. Geol. Portugal*, *9*, 9–19.

Madeira, J., J. Mata, C. Mourão, A. Brum da Silveira, S. Martins, R. Ramalho, and D. Hoffmann (2010), Volcano-stratigraphic and structural evolution of Brava Island (Cape Verde) from 40Ar/39Ar, U/Th and field constraints, *J. Volcanol. Geotherm. Res.*, *196*(3–4), 219–235.

Mata, J. (1996), Petrologia e Geoquímica das lavas da Ilha da Madeira: Implicações para os modelos de evolução mantélica, PhD thesis, Univ. de Lisboa. Lisboa, Portugal.

Mata, J., T. Boski, A. Boven, and J. Munhá (1995), Geocronologia das lavas da Madeira: Novas datações K-Ar, *Gaia*, *11*, 53–56.

Mata, J., P. E. Fonseca, S. Prada, D. Rodrigues, S. Martins, R. A. S. Ramalho, J. Madeira, M. Cachão, C. da Silva, and M. J. Matias (2013), O Arquipélago da Madeira, in *Geologia de Portugal, Geol. Meso-cenozóica*, vol. II, edited by R. Dias et al., chap. III.8.2, pp. 691–746, Escolar Editora. Lisbon, Portugal.

Michalski, J. R., M. D. Kraft, T. G. Sharp, and P. R. Christensen (2005), Palagonite-like Alteration Products on the Earth and Mars I: Spectroscopy (0.4–25 microns) of Weathered Basalts and Silicate Alteration Products, *Proc. Lunar Planet. Sci. Conf.*, 36th, 1188.

Miller, K., M. Kominz, J. Browning, J. Wright, G. Mountain, M. Katz, P. Sugarman, B. Cramer, N. Christie-Blick, and S. Pekar (2005), The Phanerozoic record of global sea-level change, *Science*, *310*(5752), 1293–1298.
Mitchell-Thomé, R. C. (1974), The sedimentary rocks of Macaronesia, *Geol. Rundsch.*, *63*(3), 1179–1216.
Moore, J. (1985), Structure and eruptive mechanisms at Surtsey Volcano, Iceland, *Geol. Mag.*, *122*(6), 649–661.
Perch-Nielsen, K. (1985), Cenozoic calcareous nannofossils, in *Plankton Stratigraphy, Cambridge Earth Sci. Ser.*, vol. 1, 2nd ed., edited by H. H. Bolli, J. B. Saunders, and K. Perch-Nielsen, pp. 329–554, Cambridge Univ. Press, Cambridge, U. K.
Petschick, R. (2004), Macdiff 4.2.5 powder diffraction software.
Ramalho, R. A. S. (2010), Building the Cape Verde islands, PhD thesis, Univ. of Bristol, Bristol, U. K.
Ramalho, R. A. S. (2011), *Building the Cape Verde Islands*, 1st ed., Springer, Berlin, Heidelberg.
Ramalho, R. A. S., G. Helffrich, M. Cosca, D. Vance, D. Hoffmann, and D. N. Schmidt (2010a), Episodic swell growth inferred from variable uplift of the Cape Verde hotspot islands, *Nat. Geosci.*, *3*(11), 774–777.
Ramalho, R. A. S., G. Helffrich, M. Cosca, D. Vance, D. Hoffmann, and D. N. Schmidt (2010b), Vertical movements of ocean island volcanoes: Insights from a stationary plate environment, *Mar. Geol.*, *275*, 84–95.
Ramalho, R. S., R. Quartau, A. S. Trenhaile, N. C. Mitchell, C. D. Woodroffe, and S. P. Ávila (2013), Coastal evolution on volcanic oceanic islands: A complex interplay between volcanism, erosion, sedimentation, sea-level change and biogenic production, *Earth Sci. Rev.*, *127*, 140–170, doi:10.1016/j.earscirev.2013.10.007.
Romariz, C. (1971a), Notas petrográficas sobre rochas sedimentares Portuguesas. XI—Os biocalcaritos neríticos de S. Vicente (Ilha da Madeira), *Boletim Museu Lab. Mineral. Geol. Faculdade Ciênc. Lisboa*, *12*(1), 27–35.
Romariz, C. (1971b), Notas petrográficas sobre rochas sedimentares Portuguesas. XII—Calcaritos afânicos da Ilha da Madeira, *Boletim Museu Lab. Mineral. Geol. Faculdade Ciênc. Lisboa*, *12*(1), 55–65.
Ryan, W. B. F., et al. (2009), Global multi-resolution topography synthesis, *Geochem. Geophys. Geosyst.*, *10*, Q03014, doi:10.1029/2008GC002332.
Santos, A., E. Mayoral, C. Da Silva, M. Cachão, M. Johnson, and B. Baarli (2011), Miocene intertidal zonation on a volcanically active shoreline: Porto Santo in the Madeira Archipelago, Portugal, *Lethaia*, *44*(1), 26–32.
Santos, A., E. Mayoral, M. E. Johnson, B. G. Baarli, C. M. da Silva, M. Cachão, and J. Ledesma-Vázquez (2012), Basalt mounds and adjacent depressions attract contrasting biofacies on a volcanically active Middle Miocene coastline (Porto Santo, Madeira Archipelago, Portugal), *Facies*, *58*(4), 573–585.
Schmidt, R., and H. Schmincke (2002), From seamount to oceanic island, Porto Santo, central East-Atlantic, *Int. J. Earth Sci.*, *91*(4), 594–614.
Schmidt, R., and H.-U. Schmincke (2000), Seamounts and island building, in *Encyclopedia of Volcanoes*, edited by H. Sigurdsson et al., pp. 383–402, Academic Press, San Diego, Calif.
Schmincke, H.-U. (2004), *Volcanism*, 1st ed., Springer, Berlin.
Serralheiro, A. (1976), A Geologia da Ilha de Santiago (Cabo Verde), *Boletim Museu Lab. Mineral. Geol. Faculdade Ciênc.*, *14*, 157–369.
Singer, A. (1974), Mineralogy of palagonitic material from the Golan Heights, Israel, *Clays Clay Miner.*, *22*, 231–240.
Sohn, Y. (1995), Geology of Tok Island, Korea: Eruptive and depositional processes of a shoaling to emergent island volcano, *Bull. Volcanol.*, *56*(8), 660–674.
Staudigel, H., and H. Schmincke (1984), The Pliocene seamount series of La Palma/Canary Islands, *J. Geophys. Res.*, *89*(B13), 11,195–11,215.
Steiger, R., and E. Jäger (1977), Subcommission on geochronology: Convention on the use of decay constants in geo-and cosmochronology, *Earth Planet. Sci. Lett.*, *36*(3), 359–362.
Stroncik, N. A., and H.-U. Schmincke (2002), Palagonite—A review, *Int. J. Earth Sci.*, *91*(4), 680–697.
Summers, K. V. (1976), Mineralogical notes—The clay component of the Columbia River palagonites, *Am. Mineral.*, *61*, 492–494.
Thorarinsson, S. (1967a), *Surtsey: The New Island in the North Atlantic*, Viking Press, N. Y.
Thorarinsson, S. (1967b), The Surtsey eruption and related scientific work, *Polar Rec.*, *13*(86), 571–578.
Thordarson, T., and O. Sigmarsson (2009), Effusive activity in the 1963–1967 Surtsey eruption, Iceland: Flow emplacement and growth of small lava shields, in edited by T. Thordarson, et al., Studies in Volcanology: The Legacy of George Walker. Spec. Publ. IAVCEI, vol. 2, pp. 53–84, Geol. Soc. London, London, U. K.
Watkins, N. D., and A. Abdel-Monem (1971), Detection of the Gilsa geomagnetic polarity event on the island of Madeira, *Geol. Soc. Am. Bull.*, *82*(1), 191–198.
Wohletz, K., and R. McQueen (1984), Experimental studies of hydromagmatic volcanism, in *Explosive Volcanism: Inception, Evolution, and Hazards*, edited by G. S. Committee, pp. 158–169, Natl. Acad. Press, Washington, D. C.
Zazo, C., J. Goy, C. Dabrio, V. Soler, C. Hillaire-Marcel, B. Ghaleb, J. González-Delgado, T. Bardají, and A. Cabero (2007), Quaternary marine terraces on Sal Island (Cape Verde archipelago), *Quat. Sci. Rev.*, *26*(7–8), 876–893.
Zbyszewski, G., and O. V. Ferreira (1962), Compte rendu de deux visites au volcan de Capelinhos (Açores) après son éruption, *Mem. Serv. Geol. Portugal*, *9*(21–25). Mem. Serv. Geol., Portugal.
Zbyszewski, G., O. V. Ferreira, A. C. Medeiros, L. Aires-Barros, L. Silva, J. Munhá, and F. Barriga (1975), Notícia Explicativa das Folhas A e B da ilha da Madeira, technical report, Serv. Geol. de Portugal, Lisbon.
Zhou, Z., W. S. Fyfe, K. Tazaki, and S. J. Vandergaast (1992), The structural characteristics of palagonite from DSDP Site 335, *Can. Minerol.*, *30*(1), 75–81.